Histopathological validation of electromechanical mapping in assessing myocardial viability in a porcine model of chronic ischemia

Yi Zheng MD, Marlos R Fernandes MD, Guilherme V Silva MD, Cristiano O Cardoso MD, John Canales MD, Amir Gahramenpour MD, Fred Baimbridge BS, Maria da Graça Cabreira-Hansen PhD, Emerson C Perin MD PhD

Y Zheng, MR Fernandes, GV Silva, et al. Histopathological validation of electromechanical mapping in assessing myocardial viability in a porcine model of chronic ischemia. Exp Clin Cardiol 2008;13(4):198-203.

BACKGROUND AND OBJECTIVE: Left ventricular electromechanical mapping (EMM) determines myocardial viability on the basis of endocardial electrograms. The aim of the present study was to validate EMM in differentiating infarcted myocardium from viable myocardium by histopathological analysis.

METHODS: Sixty days after implanting an ameroid constrictor over the left circumflex artery to create chronic ischemia in 19 pigs, EMM was performed to construct unipolar voltage (UPV), bipolar voltage (BPV) and linear local shortening (LLS) maps. Noninfarcted and infarcted myocardium were identified by histopathology. Threshold determinations comparing noninfarcted tissue with scarred tissue were made by measuring the area under the receiver operating characteristic curves.

RESULTS: From the 19 hearts, 149 myocardial segments were divided into noninfarcted myocardium (n=128) and transmural infarct (n=21). UPV, BPV and LLS values (4.7±1.2 mV, 2.8±2.5 mV and 10.0±5.1%, respectively) of infarcted segments were significantly lower than those in noninfarcted myocardium (10.9±3.4 mV, 4.5±2.4 mV and 15.7±9.5%, respectively; P<0.01 for each comparison). The threshold values of UPV, BPV and LLS differentiating noninfarcted from infarcted myocardium were 6.2 mV (98% sensitivity, 95% specificity, 97% accuracy), 2.8 mV (80% sensitivity, 72% specificity, 79% accuracy) and 12.3% (68% sensitivity, 67% specificity, 68% accuracy), respectively. The relative dispersion of voltage was lower for UPV versus BPV.

CONCLUSION: UPV can accurately differentiate infarcted from noninfarcted tissue in the chronic ischemic heart of pigs; however, BPV and LLS results were less accurate.

Key Words: *Cut-off point; Electromechanical mapping; Infarct identification; Myocardial viability; Transmural infarct*

Assessing myocardial viability is important in the evaluation and management of patients with ischemic cardiomyopathy. Moreover, quantifying the extent of viable myocardium may identify patients who could benefit from interventional therapy. The recovery of functional myocardium after revascularization appears to be directly related to the presence and the extent of scarred tissue in the heart (1). In addition, a substantial increase of viable left ventricular (LV) myocardium is needed to improve LV ejection fraction after revascularization (2). Myocardial viability has been identified by several widely used diagnostic techniques, such as single photon emission computed tomography (3-7), positron emission tomography (8,9), magnetic resonance imaging (10-12) and dobutamine stress echocardiography (13).

Electromechanical mapping (EMM) has been compared with single photon emission computed tomography (14-16), positron emission tomography (17), dobutamine stress echocardiography (18,19) and magnetic resonance imaging (20) in assessing myocardial infarction and viability. EMM has been used as a three-dimensional navigation system to guide injections during transendocardial delivery of gene or cell therapy products. Delivering therapeutic products into a noninfarcted area of tissue is critical for angiogenesis (21,22); therefore, differentiating infarcted from noninfarcted myocardium is important. Our goal was to define EMM criteria for differentiating noninfarcted from infarcted myocardial tissue using histopathology as the gold standard.

METHODS

Animal care

All animals received humane care in compliance with the Animal Welfare Act, the "Principles of Laboratory Animal Care" formulated by the National Society for Medical Research, and the "Guide for the Care and Use of Laboratory Animals" (National Institutes of Health publication number 85-23, revised 1996). The present study was performed in accordance with the standard humane care guidelines of the Institutional Animal Care and Use Committee of the Texas Heart Institute, which conform to federal guidelines.

Model of chronic ischemic cardiomyopathy

A total of 23 domestic pigs weighing 30 kg to 60 kg underwent implantation of an ameroid constrictor. After sedation and preoperative preparation, the animals were transported to the operating room and placed in the right lateral recumbent position. General anesthesia was maintained during the surgical procedure with the use of isoflurane (0.5% to 3.0%) and oxygen (40% to 100%). Respiratory rate, fraction of inspired oxygen and tidal volumes were adjusted to maintain a steady state of anesthesia. The left chest and shoulder were prepped and the

Stem Cell Center, Texas Heart Institute at St Luke's Episcopal Hospital, Houston, Texas, USA
Correspondence: Dr Emerson C Perin, Texas Heart Institute, MC 2-255, PO Box 20345, Houston, Texas 77225-0345, USA.
Telephone 832-355-9405, fax 832-355-9440, e-mail eperin@bluegate.com
Received for publication September 11, 2008. Accepted October 6, 2008

chest was opened at the fifth intercostal space. The fifth rib was removed, and the dorsal lung was wrapped and packed with gauze to expose the heart. The pericardium was then excised and the circumflex artery isolated. An ameroid constrictor (Research Instruments SW, USA) with an internal diameter of 2.25 mm to 2.75 mm was placed around the circumflex artery at its origin. If an intermediate branch was present, either a single ameroid that surrounded both arteries was used or a second ameroid was placed around the intermediate branch. After the constrictor was placed around the circumflex artery, the rib cage was closed with steel wire, and the muscle and skin layers were closed in standard fashion. After surgery, pigs were treated with antibiotics and analgesics, and maintained in the animal facility for 60 days to allow healing of the infarct. Four pigs were excluded from analysis because of early death at 26 to 47 days after ameroid implantation. Final EMM assessment was performed on the remaining 19 pigs.

EMM system

The nonfluoroscopic EMM system has been described previously (20,23-26). In brief, the EMM system (NOGA, Biosense Webster Inc, USA) comprises a triangular location pad with three coils generating ultralow magnetic field energy, a stationary reference catheter with a miniature magnetic field sensor located on the body surface, a navigation sensor mapping catheter with deflectable tip and electrodes providing endocardial signals, and a workstation for information processing and three-dimensional LV reconstruction. The maps were constructed by sequential sampling of the LV cavity. Each sample consisted of a map point that contained regional voltage and contractility information.

Mapping procedure

EMM was performed 60 days after ameroid placement. The femoral artery was exposed via a left femoral cutdown, and an 8 Fr sheath was inserted into the femoral artery. A D-type or F-type NogaStar mapping catheter was selected on the basis of LV size of each pig. Under fluoroscopic guidance, the 7 Fr catheter was advanced to the descending aorta, and then around the aortic arch and (fully deflected) across the aortic valve into the left ventricle. The deflection of the catheter was relaxed, and the tip was oriented to the LV apex. The initial map point was taken at the apex followed by points at the base of the septum and the lateral wall, thereby completing an initial triangle that defined the borders of the left ventricle. Subsequent points were taken until all endocardial segments had been uniformly sampled with at least three points in each of the 17 segments.

After acquiring sufficient points to construct the initial silhouette of the LV cavity, an automatic filter was used to remove improper data points from the original map. The following were considered unacceptable mapping points: those located in the interior of the LV cavity, those that did not fit the standard stability criteria (location stability less than 4 mm, loop stability less than 6 mm, cycle length less than 10%), those obtained during a premature ventricular contraction, and those unrelated to the LV cavity (eg, in an atrial location). Using the above-described criteria, each point was filtered online immediately after acquisition and during the postprocessing analysis. Each map was displayed in a polar distribution format (bull's eye). The average of the results of unipolar voltage (UPV), bipolar voltage (BPV) and linear local shortening (LLS) was correlated with the histopathological analysis of each individual segment (Figures 1A, 1B and 1C).

Histopathological analysis

After completing the mapping study, the pigs were humanely euthanized under deep anesthesia. The hearts were removed from each pig and perfusion fixed under physiological pressure with 10% neutral buffered formalin. According to American Heart Association segmentation criteria (27), the hearts were cut into 17 segments. A gross description of the infarcted area and the depth of the infarct was recorded for each segment. Myocardial sections were transferred to a 15% sucrose solution, dehydrated in a graded series of alcohols and embedded in paraffin. Sections (4 μm to 5 μm) were mounted on charged slides and stained with hematoxylin and eosin, and Masson's trichrome to visualize fibrosis and scarring. Based on both gross and histological analyses, the hearts were categorized as noninfarcted myocardium and transmural scar (infarcted tissue involving more than 50% of the myocardial thickness) for each segment (Figures 1D and 1E).

Comparison of EMM results and histopathology

By using NOGA software, an American Heart Association 17 segment bull's eye map of voltage (unipolar and bipolar) and LLS was generated that matched histopathology segmentation. Segment by segment, the histopathology results were compared with the corresponding voltage and LLS values. Based on histology, EMM results were divided into two groups: noninfarcted and infarcted segments.

Statistical analysis

Data are presented as the mean ± SD. The Wilcoxon's rank-sum test was used to compare the two groups of segments. Thresholds comparing noninfarcted with infarcted tissue were determined using area under the receiver operating characteristic curves. $P<0.05$ was considered to be statistically significant.

RESULTS

For each of the 19 pigs in the study, 92±14 points were acquired (total mapping time 49±21 min). Of the 152 segments from the left circumflex territory (lateral and posterior segments), three segments were excluded because they were derived from fewer than three EMM points, resulting in a total of 149 segments for analysis: 128 segments of noninfarcted myocardium and 21 segments with infarcted myocardium. The values for UPV, BPV and LLS were significantly lower for infarcted segments than for noninfarcted segments (Table 1). Results of receiver operating characteristics (Figures 2, 3 and 4) showed that the threshold for distinguishing between infarcted and noninfarcted myocardium was 6.2 mV for UPV (sensitivity 98%, specificity 95%, accuracy 97%), 2.8 mV for BPV (sensitivity 80%, specificity 72%, accuracy 79%) and 12.3% for LLS (sensitivity 68%, specificity 67%, accuracy 68%). Both BPV and LLS were less accurate than UPV in differentiating infarcted segments from noninfarcted segments because of a larger relative dispersion (SD/mean) in BPV and LLS than in UPV (Table 2).

DISCUSSION

Our study confirms that EMM can be used to distinguish infarcted from noninfarcted myocardium in the porcine model

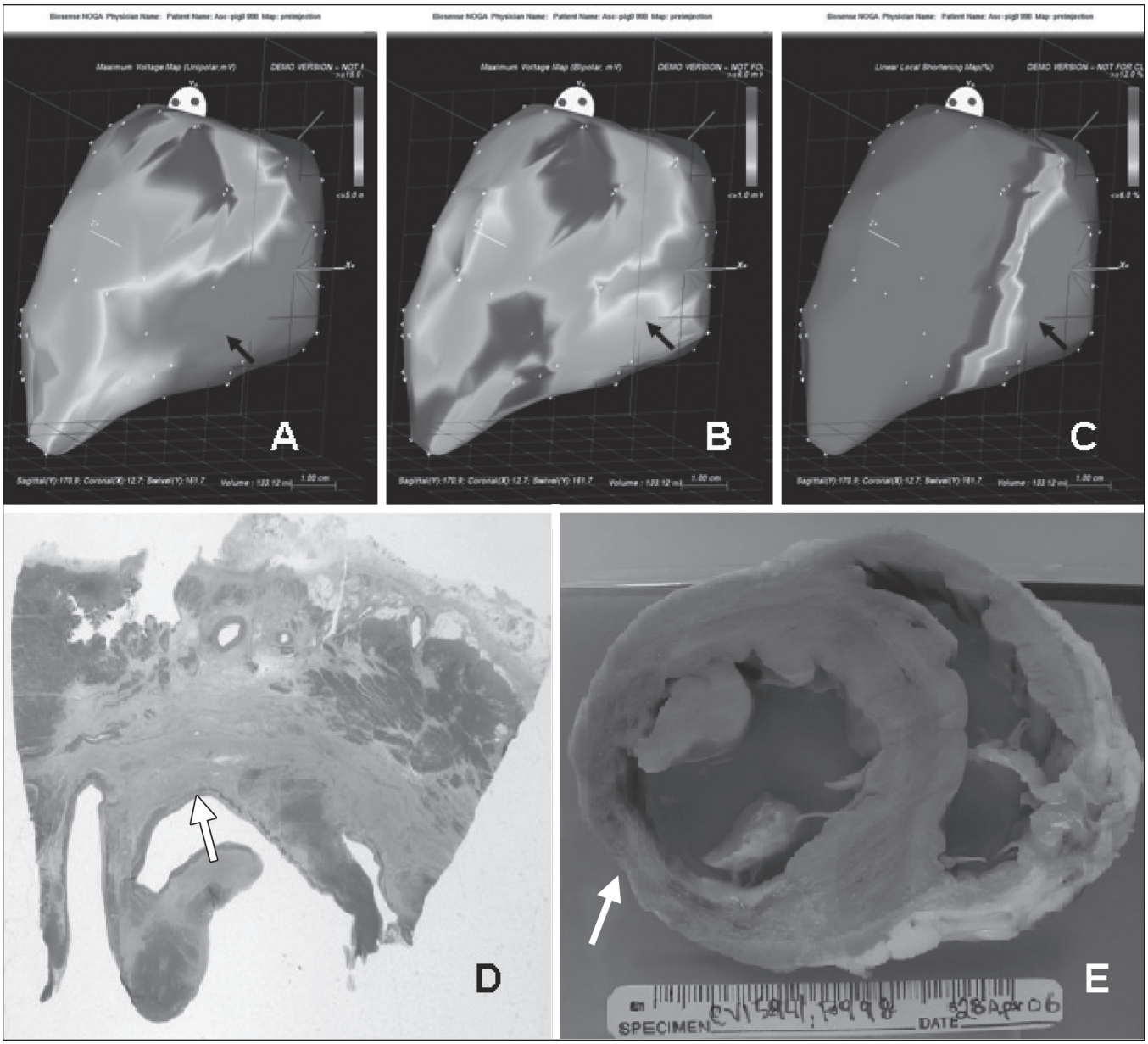

Figure 1) *Unipolar voltage (***A***), bipolar voltage (***B***) and linear local shortening (LLS) (***C***) maps showing an area of inferior-mid transmural infarction (black arrows) on left lateral view. Accordingly, histological slides (***D***, stained with hematoxylin and eosin, and Masson's trichrome) and gross specimen (***E***) from the same animal show transmural scar (white arrows)*

TABLE 1
Electrical data in 149 segments classified according to histopathological assessment

	Noninfarct (n=128)	Transmural scar (n=21)	P
Unipolar voltage, mV	10.9±3.4	4.7±1.2	0.0001
Bipolar voltage, mV	4.5±2.4	2.8±2.5	<0.0001
Linear local shortening, %	15.7±9.5	10.0±5.1	0.0012

of chronic ischemia, and contributes to previous findings by establishing a practical 'cut-off' value for distinguishing noninfarcted myocardium from scar.

The porcine ameroid model of chronic myocardial ischemia has been widely used to evaluate the outcome of therapeutic angiogenesis (28,29) and stem cell therapy (30). The advantage of the ameroid model, unlike the model of acute myocardial infarction induced by coronary balloon occlusion or ligation, is that it provides an ischemic area with patches of scar tissue. The histopathological result from the present study confirmed this ischemia-infarct mixed model and allowed us to set up a threshold in EMM to distinguish infarcted myocardium.

The ability of EMM to diagnose myocardial ischemia and viability has been extensively studied in both preclinical and clinical studies (15,20,31,32). However, using EMM characteristics (UPV, BPV and LLS) to differentiate scar from noninfarcted myocardium, with histopathology as the gold standard, has been assessed in few studies. Callans et al (18) demonstrated that decreased endocardial electrocardiogram amplitude could

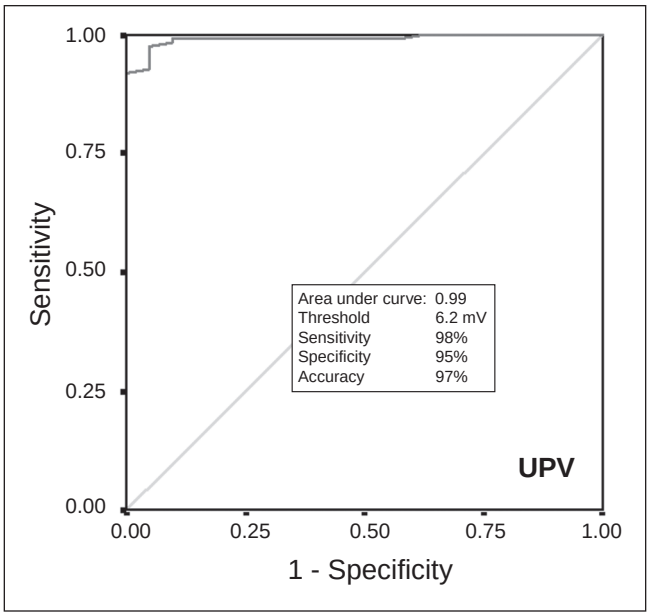

Figure 2) *Receiver operating characteristic comparing unipolar voltage (UPV) of noninfarcted myocardium with transmural scar*

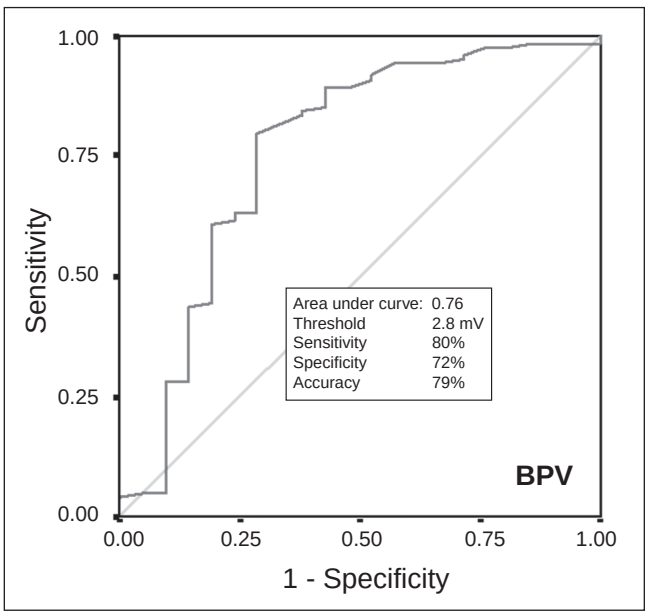

Figure 3) *Receiver operating characteristic comparing bipolar voltage (BPV) of noninfarcted myocardium with transmural scar*

be used as a good predictor to identify the infarcted area in a porcine model of healed (six to 10 weeks after acute infarction) anterior myocardial infarction. Wolf et al (33) and Gepstein et al (34) used the NOGA system to differentiate infarcted from noninfarcted myocardium in a canine model of chronic anterior wall infarction by permanent LAD ligation.

Fallavollita et al (35) demonstrated the presence of endocardial voltage amplitude spatial heterogeneity in normal and chronically dysfunctional myocardium. The authors showed that in normal hearts the voltage of the inferior wall is lower than that of the anterior wall. In our study, we created chronic ischemia by placing an ameroid over the left circumflex artery. To avoid the confounding factor of UPV spatial heterogeneity,

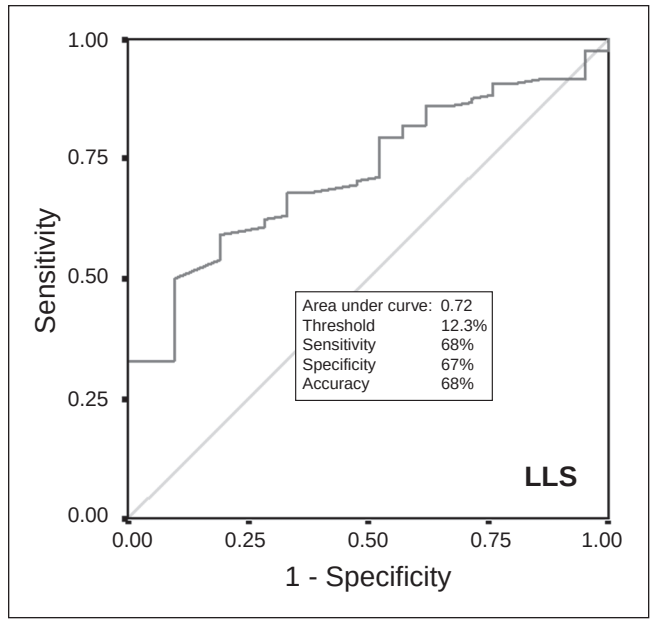

Figure 4) *Receiver operating characteristic comparing linear local shortening (LLS) of noninfarcted myocardium and transmural scar*

TABLE 2
Relative dispersion (SD/mean) of voltage and linear local shortening in 149 segments

	Noninfarct (n=128)	Transmural scar (n=21)
Relative dispersion, %		
Unipolar voltage	31.2	25.5
Bipolar voltage	53.3	89.3
Linear local shortening	60.5	51.0

we limited our analyses of NOGA and pathology to the lateral and inferior walls where the ameroid had induced myocardial ischemia.

Some studies (18,33,34) have suggested that BPV amplitude is superior to UPV amplitude for identifying myocardial viability. However, Fallavollita et al (35) reported that BPV has greater variability among both normal and infarcted regions than does UPV. Our results also showed that in both infarcted and noninfarcted regions, BPV had greater variability than UPV. Compared with unipolar measurement, the bipolar electrogram offers the theoretical advantage of minimizing the effects of far-field averaging that would reduce relative differences in the electrogram voltage. However, BPV amplitude is very angle-dependent. This angle dependency means that if the activation front from the endocardium is perpendicular to the electrode pair, the bipolar spike will be of maximum amplitude, whereas if it is parallel, both electrodes will record the same waveform at the same time, and no spike will result (36,37). In our study, UPV was more reproducible than BPV, and this may be why UPV is used in most clinical cell therapy studies (15,20,38,39).

Cell therapy for the treatment of cardiovascular disease has generated promising results, which, in turn, have stimulated an interest in studying optimal delivery methods. Although intracoronary delivery provides a homogeneous distribution of cells to the area of interest, cell retention rates may be lower with

intracoronary delivery than with intramyocardial injections (40). Depending on patient circumstances, the cell or gene product may have to be delivered directly to ischemic myocardium to promote angiogenesis or to infarcted segments to promote myogenesis. Therefore, the ability to precisely differentiate noninfarcted myocardium from scar in the catheterization laboratory is important for guiding cell and gene therapy to specific myocardial regions.

In the present study, we determined a UPV threshold value for differentiating infarcted from noninfarcted myocardium, and this value was validated by histopathological assessment. Using this threshold value, practitioners can use EMM as a guiding system to accurately inject cell or gene products into noninfarcted or infarcted myocardium for achieving angiogenesis or myogenesis.

Study limitations

Although the chronic ischemia induced in the pig model reproduces histopathological changes seen in human myocardium and produces similar changes seen in previous clinical studies, we cannot directly extrapolate results from an animal model to human cases. Moreover, to confirm the presence of viable myocardium, recovery of myocardial contractility after restoration of blood flow must be demonstrated. Noninfarcted segments detected by histopathological assessment contained normal myocardium and chronically dysfunctional (hibernating) myocardium, and diminished the predicted value of LLS. Identifying hibernating myocardium by an additional imaging modality, such as stress echocardiography, should be included in future studies.

CONCLUSION

Using histopathology as the gold standard, we have shown that electromechanical parameters can distinguish noninfarcted myocardium from transmural scar with high sensitivity and specificity. Our results establish a practical cut-off point that can be used to identify myocardial segments compromised by transmural myocardial infarction.

REFERENCES

1. Depre C, Vanoverschelde JL, Melin JA, et al. Structural and metabolic correlates of the reversibility of chronic left ventricular ischemic dysfunction in humans. Am J Physiol 1995;268:H1265-75.
2. Bax JJ, Poldermans D, Elhendy A, et al. Improvement of left ventricular ejection fraction, heart failure symptoms and prognosis after revascularization in patients with chronic coronary artery disease and viable myocardium detected by dobutamine stress echocardiography. J Am Coll Cardiol 1999;34:163-9.
3. Ragosta M, Beller GA, Watson DD, Kaul S, Gimple LW. Quantitative planar rest-redistribution 201Tl imaging in detection of myocardial viability and prediction of improvement in left ventricular function after coronary bypass surgery in patients with severely depressed left ventricular function. Circulation 1993;87:1630-41.
4. Udelson JE, Coleman PS, Metherall J, et al. Predicting recovery of severe regional ventricular dysfunction. Comparison of resting scintigraphy with 201Tl and 99mTc-sestamibi. Circulation 1994;89:2552-61.
5. Perrone-Filardi P, Pace L, Prastaro M, et al. Assessment of myocardial viability in patients with chronic coronary artery disease. Rest-4-hour-24-hour 201Tl tomography versus dobutamine echocardiography. Circulation 1996;94:2712-9.
6. Qureshi U, Nagueh SF, Afridi I, et al. Dobutamine echocardiography and quantitative rest-redistribution 201Tl tomography in myocardial hibernation. Relation of contractile reserve to 201Tl uptake and comparative prediction of recovery of function. Circulation 1997;95:626-35.
7. Dakik HA, Howell JF, Lawrie GM, et al. Assessment of myocardial viability with 99mTc-sestamibi tomography before coronary bypass graft surgery: Correlation with histopathology and postoperative improvement in cardiac function. Circulation 1997;96:2892-8.
8. Bax JJ, Patton JA, Poldermans D, Elhendy A, Sandler MP. 18-Fluorodeoxyglucose imaging with positron emission tomography and single photon emission computed tomography: Cardiac applications. Semin Nucl Med 2000;30:281-98.
9. Maes A, Flameng W, Nuyts J, et al. Histological alterations in chronically hypoperfused myocardium. Correlation with PET findings. Circulation 1994;90:735-45.
10. Kim RJ, Wu E, Rafael A, et al. The use of contrast-enhanced magnetic resonance imaging to identify reversible myocardial dysfunction. N Engl J Med 2000;343:1445-53.
11. Stillman AE, Wilke N, Jerosch-Herold M. Myocardial viability. Radiol Clin North Am 1999;37:361-78.
12. Klein C, Nekolla SG, Bengel FM, et al. Assessment of myocardial viability with contrast-enhanced magnetic resonance imaging: Comparison with positron emission tomography. Circulation 2002;105:162-7.
13. Hayat SA, Senior R. Contrast echocardiography for the assessment of myocardial viability. Curr Opin Cardiol 2006;21:473-8.
14. Kornowski R, Hong MK, Gepstein L, et al. Preliminary animal and clinical experiences using an electromechanical endocardial mapping procedure to distinguish infarcted from healthy myocardium. Circulation 1998;98:1116-24.
15. Fuchs S, Hendel RC, Baim DS, et al. Comparison of endocardial electromechanical mapping with radionuclide perfusion imaging to assess myocardial viability and severity of myocardial ischemia in angina pectoris. Am J Cardiol 2001;87:874-80.
16. Kornowski R, Hong MK, Leon MB. Comparison between left ventricular electromechanical mapping and radionuclide perfusion imaging for detection of myocardial viability. Circulation 1998;98:1837-41.
17. Koch KC, vom Dahl J, Wenderdel M, et al. Myocardial viability assessment by endocardial electroanatomic mapping: Comparison with metabolic imaging and functional recovery after coronary revascularization. J Am Coll Cardiol 2001;38:91-8.
18. Callans DJ, Ren JF, Michele J, Marchlinski FE, Dillon SM. Electroanatomic left ventricular mapping in the porcine model of healed anterior myocardial infarction. Correlation with intracardiac echocardiography and pathological analysis. Circulation 1999;100:1744-50.
19. Lessick J, Hayam G, Zaretsky A, Reisner SA, Schwartz Y, Ben-Haim SA. Evaluation of inotropic changes in ventricular function by NOGA mapping: Comparison with echocardiography. J Appl Physiol 2002;93:418-26.
20. Perin EC, Silva GV, Sarmento-Leite R, et al. Assessing myocardial viability and infarct transmurality with left ventricular electromechanical mapping in patients with stable coronary artery disease: Validation by delayed-enhancement magnetic resonance imaging. Circulation 2002;106:957-61.
21. Kleiman NS, Patel NC, Allen KB, et al. Evolving revascularization approaches for myocardial ischemia. Am J Cardiol 2003;92:9N-17N.
22. Kinnaird T, Stabile E, Epstein SE, Fuchs S. Current perspectives in therapeutic myocardial angiogenesis. J Interv Cardiol 2003;16:289-97.
23. Gepstein L, Hayam G, Ben-Haim SA. A novel method for nonfluoroscopic catheter-based electroanatomical mapping of the heart. In vitro and in vivo accuracy results. Circulation 1997;95:1611-22.
24. Gepstein L, Hayam G, Shpun S, Ben-Haim SA. Hemodynamic evaluation of the heart with a nonfluoroscopic electromechanical mapping technique. Circulation 1997;96:3672-80.
25. Ben-Haim SA, Osadchy D, Schuster I, Gepstein L, Hayam G, Josephson ME. Nonfluoroscopic, in vivo navigation and mapping technology. Nat Med 1996;2:1393-5.
26. Perin EC, Silva GV, Sarmento-Leite R, Vaughn WK, Fish RD, Ferguson JJ 3rd. Left ventricular electromechanical mapping: Preliminary evidence of electromechanical changes after successful coronary intervention. Am Heart J 2002;144:693-701.

27. Cerqueira MD, Weissman NJ, Dilsizian V, et al. Standardized myocardial segmentation and nomenclature for tomographic imaging of the heart. A statement for healthcare professionals from the Cardiac Imaging Committee of the Council on Clinical Cardiology of the American Heart Association. Int J Cardiovasc Imaging 2002;18:539-42.
28. Mack CA, Patel SR, Schwarz EA, et al. Biologic bypass with the use of adenovirus-mediated gene transfer of the complementary deoxyribonucleic acid for vascular endothelial growth factor 121 improves myocardial perfusion and function in the ischemic porcine heart. J Thorac Cardiovasc Surg 1998;115:168-76.
29. Tio RA, Tkebuchava T, Scheuermann TH, et al. Intramyocardial gene therapy with naked DNA encoding vascular endothelial growth factor improves collateral flow to ischemic myocardium. Hum Gene Ther 1999;10:2953-60.
30. Bhakta S, Greco NJ, Finney MR, et al. The safety of autologous intracoronary stem cell injections in a porcine model of chronic myocardial ischemia. J Invasive Cardiol 2006;18:212-8.
31. Botker HE, Lassen JF, Hermansen F, et al. Electromechanical mapping for detection of myocardial viability in patients with ischemic cardiomyopathy. Circulation 2001;103:1631-7.
32. Fuchs S, Kornowski R, Shiran A, Pierre A, Ellahham S, Leon MB. Electromechanical characterization of myocardial hibernation in a pig model. Coron Artery Dis 1999;10:195-8.
33. Wolf T, Gepstein L, Dror U, et al. Detailed endocardial mapping accurately predicts the transmural extent of myocardial infarction. J Am Coll Cardiol 2001;37:1590-7.
34. Gepstein L, Goldin A, Lessick J, et al. Electromechanical characterization of chronic myocardial infarction in the canine coronary occlusion model. Circulation 1998;98:2055-64.
35. Fallavollita JA, Valeti U, Oza S, Canty JM Jr. Spatial heterogeneity of endocardial voltage amplitude in viable, chronically dysfunctional myocardium. Basic Res Cardiol 2004;99:212-22.
36. Ideker RE, Smith WM, Blanchard SM, et al. The assumptions of isochronal cardiac mapping. Pacing Clin Electrophysiol 1989;12:456-78.
37. Clement E. über eine neue Mwthode zur Untersuchung der Fortleitung des Erregungsvorgages im Herzen. Zeitschrift Für biologie 1912;58:110-61.
38. Samady H, Liu YH, Choi CJ, et al. Electromechanical mapping for detecting myocardial viability and ischemia in patients with severe ischemic cardiomyopathy. Am J Cardiol 2003;91:807-11.
39. Kornowski R, Hong MK, Leon MB. Direct myocardial revascularization in ischemic heart disease. Int J Cardiovasc Intervent 1998;1:3-9.
40. Hou D, Youssef EA, Brinton TJ, et al. Radiolabeled cell distribution after intramyocardial, intracoronary, and interstitial retrograde coronary venous delivery: Implications for current clinical trials. Circulation 2005;112(9 Suppl):I150-6.